INTERNATIONAL DESIGN CONFERENCE - DESIGN 2002
Dubrovnik, May 14 - 17, 2002

ENERGY LOSSES DUE TO FRICTION IN GEARS

Liviu Palaghian, Mioara Bucsa and Iulian Barsan

Keywords: gears, worm gears, friction coefficient, energy losses

1. Introduction

It is well known the fact that along the action line (Og-**figure 1**) the contact between the teeth flanks is characterized by rolling with sliding [Merrit 1946, Buckingham 1949]. Only the pitch point, C, is characterized by pure rolling. This leads to energy loss by friction. The biggest values for sliding ($\xi_1(g)$ and $\xi_2(g)$) are near the foot of the tooth and the smallest are near the head of the tooth.

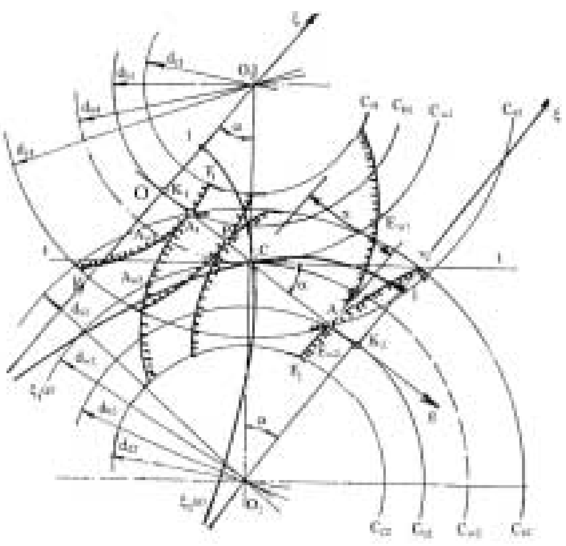

Figure 1. Theoretical contact between the teeth flanks

2. Profiles sliding at spur gears

When the normal force, F_n, is transmitted along the action line, K_1K_2, between the teeth flanks appears a sliding speed:

$$v = (\omega_1 + \omega_2) \cdot x \tag{1}$$

Where: ω_1, ω_2 - rotate speeds of the gear wheels;
x - sliding distance.
The power consumed by friction will be:

$$P_f = \mu \cdot F_n \cdot (\omega_1 + \omega_2) \cdot x \tag{2}$$

Where: μ - friction coefficient.

The meshing point, P, moves along the line of action with a speed given by:

$$\frac{dx}{dt} = r_{b1} \cdot x \tag{3}$$

Where: r_{b1} - the base circle radius.

Thus the elementary energy loss by friction will be:

$$dW = \mu \cdot F_n \cdot (\omega_1 + \omega_2) \cdot xdt = \mu \cdot F_n \cdot (\omega_1 + \omega_2) \cdot x \cdot \frac{1}{r_{b1} \cdot \omega_1} dx \tag{4}$$

In the above equation the friction coefficient is assumed to be constant while the contact moves on the line of action [Buckingham 1949].

Due to the interaction between the friction force, $\mu \cdot F_n$, and the normal force, F_n, supplementary reactions, $F_n^{'}$, will appear. They will modify the line of action position from the theoretical one, K_1K_2, in two real segments:

- The approach region, $K_1^{'}K_2^{'}$, and
- The recess region, $K_1^{''}K_2^{''}$ (**figure 2**) [Tsuniji 1997].

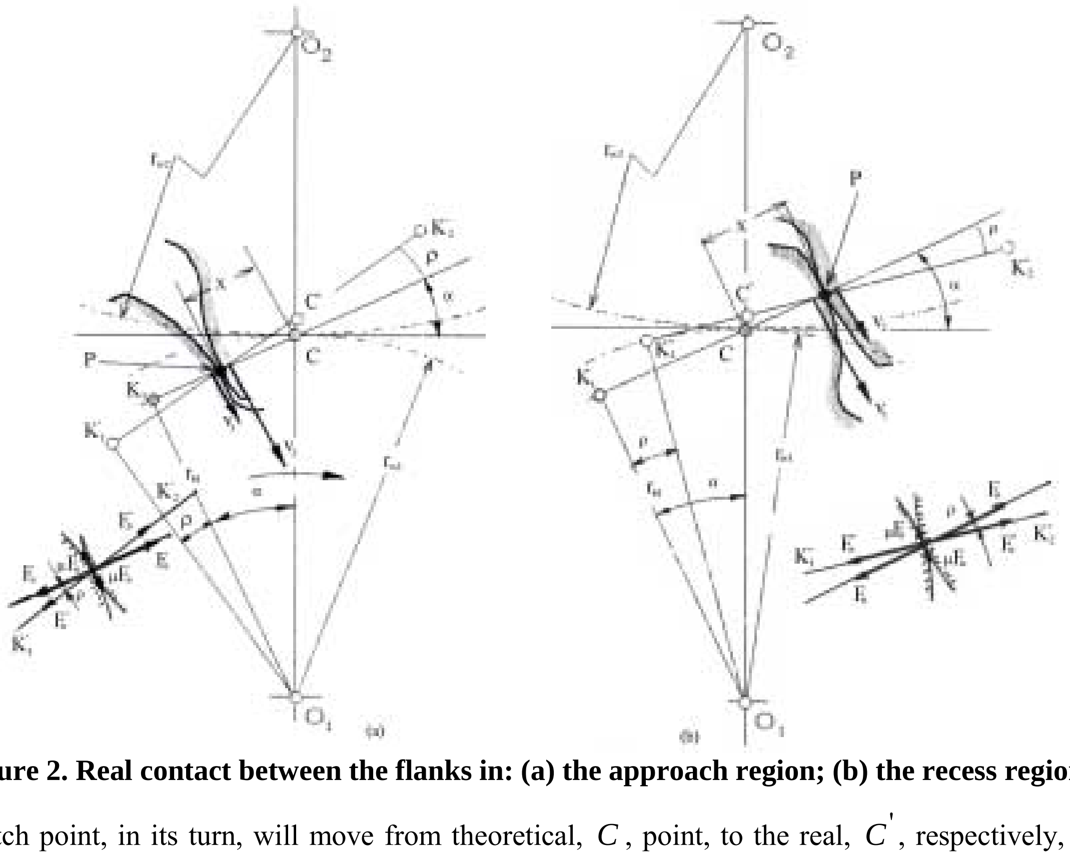

Figure 2. Real contact between the flanks in: (a) the approach region; (b) the recess region

The pitch point, in its turn, will move from theoretical, C, point, to the real, $C^{'}$, respectively, $C^{''}$, points where $K_1^{'}K_2^{'}$ and $K_1^{''}K_2^{''}$ segments intersect the centerline, O_1O_2.

This movement is a frictional one having a friction angle:

$$\rho = \mathrm{a}\tan(\mu) \tag{5}$$

The friction angle is very small, so $CC^{'}$ and $CC^{''}$ segments can be approximated with: $x \cdot \rho$.

In the above equation the maximal values for x correspond to the approach point A_1, respectively to the recess point A_2.

If the pitch point has a modified position on the centerline the rolling circles of the two gear wheels will have different radii. The pitch point moves towards the center of the driven wheel, O_2, thus the radii of the rolling circles will be:

- r'_{w1} and r'_{w2} for the C' position,
- r''_{w1} and r''_{w1} for the C'' position.

In consequence the gear ratio will have a modified value from i corresponding to C point, to i' for C' and, respectively i'' for C''.
The modifying of the gear drive kinematics will lead to an energy balance modification and, in its turn, the machine efficiency will change.

3. Profiles sliding at worm gears

In an axial plane of a worm gear, having an arhimedic worm, the gearing is similar to the rack-and-gear drive (**figure 3**) [Dobrovolski, Zablonski, Radchik, Erlij 1980].
The worm wheel is wrapping the worm and that is why in different axial planes there are different lines of action (cb line in **figure 3**). All of these lines are generating the surface of contact. The intersection between the surface of action and the worm wheel teeth, respective the worm thread is represented by the meshing line. The envelope surface of meshing lines, within the surface of action, determines the field of action (**figure 3** shows the field of action, $aca'b$, in horizontal view). The friction forces are intersecting this field.

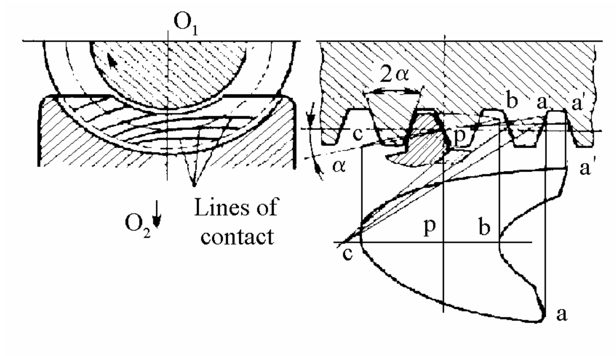

Figure 3. In axial plane the worm gear is similar to rack-and-gear

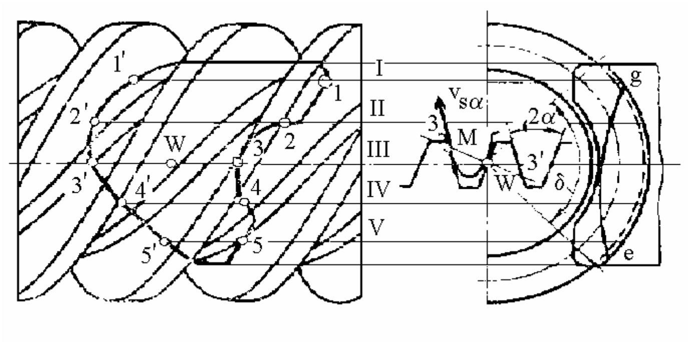

Figure 4. Between the tooth flanks of the worm wheel and the worm helix there is a sliding with rolling movement

In consequence the sliding with rolling speed between the tooth flanks of the worm wheel and the worm helix (**figure 4**) in the axial plane is [Zablonski 1985]:

$$v_{s\alpha} = \overline{WM} \cdot \omega_2 \tag{6}$$

Where: ω_2 - rotate speed of the worm wheel.

If g is the maximum value of the $\overline{WM}$ segment and F_n is the normal load along the line of action then the elementary loss of energy due to friction will be, [Townsend 1992]:

$$dW = s \cdot \mu_1 \cdot F_n \cdot v_{s\alpha} \cdot dt \tag{7}$$

Where: dt - time;

s - number of starts;

μ_1 - rolling with sliding friction coefficient;

$v_{s\alpha}$ - speed of the meshing point M on the line of action, done by:

$$v_{s\alpha} = \frac{dg}{dt} = r_{b2} \cdot \omega_2 \tag{8}$$

Where: r_{b2} - the worm wheel base circle radius.

The loss of energy due to sliding with rolling is:

$$W_1 = s\int_0^g \mu_1 F_n v_{s\alpha} \frac{1}{r_{b2}\omega_2} dg = s\int_0^g \mu_1 F_n g \frac{1}{r_{b2}} dg \tag{9}$$

The losses of power due to sliding friction along the worm thread is:

$$\Delta P = P\left[1 - \frac{\tan\gamma}{\tan(\gamma + \varphi)}\right] \tag{10}$$

Where: γ - the pitch helix angle;

$\varphi = a\tan\mu_2$; (μ_2 - sliding friction coefficient)

P - total incoming power of the worm gear.

So, in the case of a worm gear the elementary losses of energy will be:

$$dW = \Delta P \cdot dt + sk\mu_2 F_n v_{s\alpha} dt \tag{11}$$

Where k is a factor smaller than the unit: $k = \frac{\mu_1}{\mu_2}$ can be experimentally determined.

4. Experimental results

Beside the pitch point the movement between the teeth flanks is rolling with sliding. The friction coefficient of the two surfaces in contact could be determined by simulating the process on a wheel specimen. The tests were run on a "back-to-back" testing rig [Panturu 1985]. In the case of cylindrical gear the specimens were cylindrical, made of OLC 45 steel. There have been tested two couples of materials in the case of the worm gear: FcA_2 antifriction cast iron - OLC 45 steel and CuSn12T bronze - OLC 45 steel. The gear drive was lubricated with TIN EP 210 lubricant.

In the care of cylindrical gearing simulation the testing conditions were:

- four levels of specific sliding (%): 0, 12.5, 25, 37.5;
- three levels of rotate speed (rpm): 43, 100, 256;
- ten levels of external load (daN): 738, 993, 1375, 1758, 2013, 2140, 2650, 3160, 3926, 5200.

The plots presented in **figures nr. 5, 6, 7** show the real evolution of the friction coefficient versus external load for the four levels of specific sliding when the rotate speed was constant. It can be observed that the friction coefficient is lightly modified when the load increases. The coefficient increases while the rotate speed decreases. The average value of the friction coefficient goes from 0,09 at 265 rpm, to 0,11 at 100 rpm and 0,13 at 43 rpm.

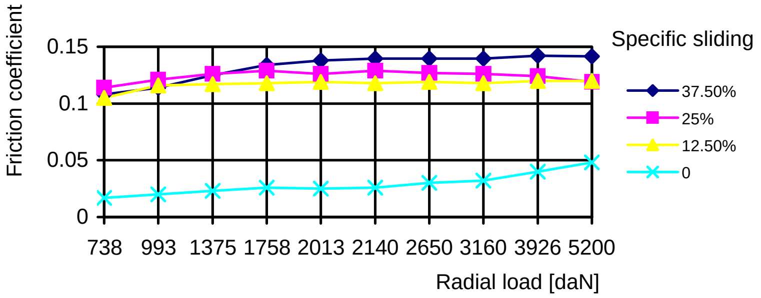

Figure 5. The friction coefficient at 43 rpm

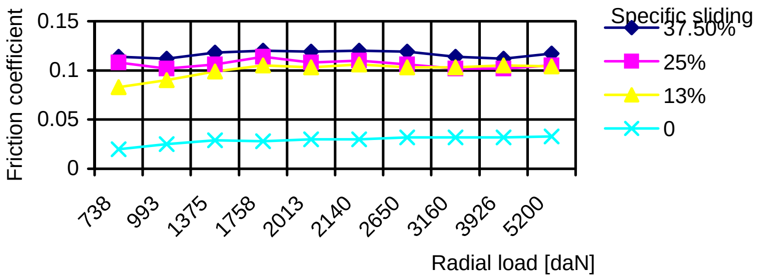

Figure 6. The friction coefficient at 100 rpm

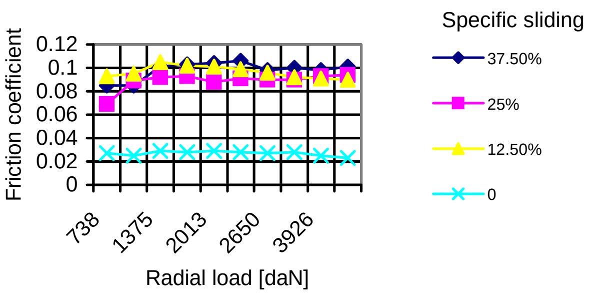

Figure 7. The friction coefficient at 256 rpm

In the case of the worm gearing simulation two types of tests were performed:
rolling with sliding tests, in this case the specimens had a cylindrical shape,
sliding tests, in this case Falex-type specimens were tested.

Testing results are presented as follows:

- **Figure 8** show the variation of the sliding with rolling friction coefficient, μ_1 versus specific sliding for different values of the normal load, for cast iron - steel couple (**fig. 8a**), respectively bronze - steel couple (**fig. 8b**).
- **Figure 9** show the variation of the sliding friction coefficient (μ_2) versus normal load for different sliding speeds, for both couples of materials.

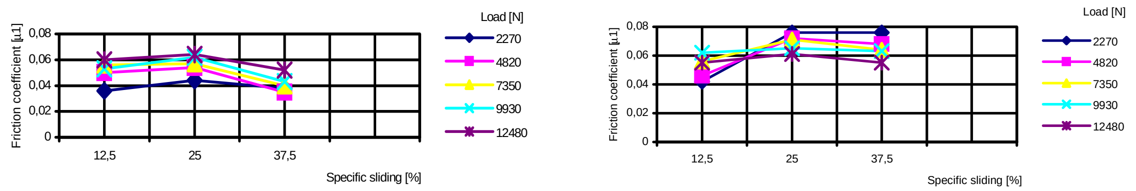

(a) (b)

Figure 8. Friction coefficient μ_1 for: (a) material couple FcA$_2$ antifriction cast iron - OLC 45 steel; (b) material couple FcA$_2$ antifriction cast iron - OLC 45 steel

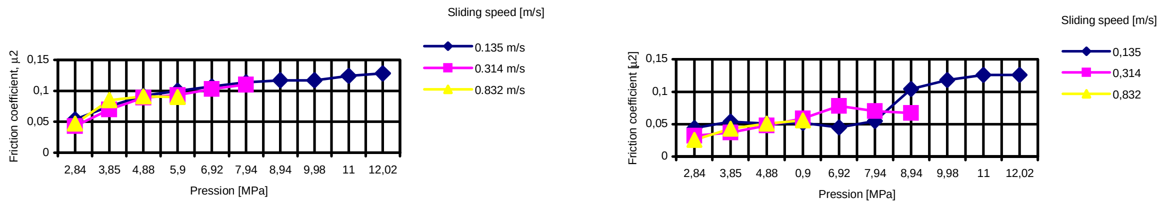

(a) (b)

Figure 9. Friction coefficient μ_2 for: (a) material couple FcA$_2$ antifriction cast iron - OLC 45 steel; (b) material couple FcA$_2$ antifriction cast iron - OLC 45 steel

5. Conclusions

Due to rolling with sliding movement tribological processes appear between the teeth surfaces in contact that lead to cinematic modifications, dynamic balance changes, supplementary forces in joints and though losses of power. At the worm gear the accurate determination of the losses of energy should include the sliding with rolling movement between the worm thread and the worm wheel teeth. This is a part from the sliding friction.

Experimental determination of the friction coefficient evolution during the teeth contact along the contact line allow the precise evaluation of the losses of power and the use of proper tribological conditions in order to reduce the losses.

References

Merrit, H. E., "Gears", Sir Isaac Pitman and sons (1946), p. 238-246

Buckingham, E., "Analytical Mechanics of Gears", McGrawHill (1949), p. 395-406

Tsuniji Yada, "Rewiew of Gear Efficiency Equation and Force Treatment", JSME International Journal, Series C, vol. 40 (1997) 1, p. 1-8.

Dobrovolski, Zablonski, K. J., Radchik, A., Erlij, E., "Elementos de maquinas", Editorial Mir. Moscou, 1980

Zablonski, K. J., "Detali masin", Jzd. Visaia scoal, Kiev, 1985

Townsend, D.P., "Gear Handbook", 2-nd edition, McGraw Hill, New York, p 12.4-12.13. 1992

Panturu, D., "The influence of speed on film thickness for rolling and rolling with sliding tribomodels in the case of linear Hertzian contact", The 5-th Conference on friction, lubrication and wear, Bucharest, 1985, p. 156-159.

Prof. Palaghian Liviu
University Dunarea De Jos, Galati, Romania, 6200 Galati 47, Domneasca Str.
Tel.: 040 36 414871
Email: liviu.palaghian@ugal.ro